Tu A16

Multiphase Flows - Nonlinear Monotone FV Scheme and Dynamic Grids

K.D. Nikitin* (Institute of Numerical Mathematics RAS), K.M. Terekhov (Institute of Numerical Mathematics RAS) & Y.V. Vassilevski (Institute of Numerical Mathematics RAS)

SUMMARY

We consider development of the nonlinear monotone FV scheme and its application to two- and three-phase flow models. The scheme is applicable for full anisotropic discontinuous permeability tensors and arbitrary conformal polyhedral cells.

The nonlinear scheme is compared with conventional linear approaches: two-point and O-scheme multipoint flux approximations. The new nonlinear scheme has a number of important advantages over the traditional linear discretizations.

Compared to the linear TPFA, the nonlinear scheme demonstrates low sensitivity to grid distortions and provides appropriate approximation in case of full anisotropic permeability tensor. For non-orthogonal grids or full anisotropic permeability tensors the conventional linear TPFA provides no approximation, while the nonlinear flux is still first-order accurate. The computational work for the new method is higher than the one for the conventional TPFA, yet it is rather competitive.

Compared to MPFA, the new scheme provides sparser algebraic systems and thus is less computational expensive. Moreover, it is monotone which means that the discrete solution preserves the non-negativity of the differential solution.

We consider using of the dynamic octree-based grids for better recovery of pressure gradient and saturation fronts propagation.

Introduction

The solution of problems arising in reservoir simulation requires two types of discretization. First, we discretize the computational domain which describes the reservoir. Second, we discretize the system of differential equations which describe the behaviour of fluids. Underground reservoirs have complex structures and unstructured meshes are in demand by the reservoir engineering community. The demand of an accurate conservative method applicable to general conformal meshes and anisotropic tensor diffusion (permeability) coefficients is very distinct as well.

There is a number of well-known conservative linear methods on unstructured meshes, including the multi-point flux approximation (MPFA), the mixed finite element (MFE) and the mimetic finite difference (MFD) methods. They are second-order accurate and are not monotone (do not preserve discrete solution non-negativity) even when the diffusion coefficient is moderately (1:100) anisotropic. The cell-centered finite volume (FV) method with a linear two-point flux approximation is monotone but not even first-order accurate for anisotropic problems or unstructured meshes. Nevertheless, this method is conventional in modeling flows in porous media due to technological simplicity and monotonicity.

A new research direction pioneered by Le Potier in LePotier (2005) uses a two-point flux stencil with two coefficients that depend on the concentrations in neighboring cells. Nonlinear FV schemes with the two-point flux approximation (TPFA) proposed in Danilov and Vassilevski (2009); Kapyrin (2007); LePotier (2005); Lipnikov et al. (2009, 2010); Nikitin and Vassilevski (2010); Yuan and Sheng (2008) guarantee solution non-negativity for general tensor coefficients on general meshes.

The method was later extended to satisfy the discrete maximum principle (DMP). For general meshes and coefficients the DMP requires a nonlinear multi-point flux approximation. For diffusion problems, such schemes were proposed in LePotier (2008); Yuan and Sheng (2011) using auxiliary unknowns at mesh vertices. Later an interpolation-free multi-point nonlinear approximation of diffusive fluxes was proposed for two-dimensional Lipnikov et al. (2012) and three-dimensional cases Chernyshenko (2013a); Gao and Wu (2013). The resulting scheme has the minimal stencil and reduces to the classical two-point FV scheme for scalar (and, in a few cases, diagonal tensor) coefficients on Voronoi or rectangular meshes.

We consider the application of the original monotone scheme Danilov and Vassilevski (2009) for multiphase flow models Nikitin et al. (2013) and dynamic grids Terekhov and Vassilevski (2013).

The nonlinear monotone two-point flux discretization has a number of important advantages over traditional linear two-point flux discretization. First, it demonstrates very low sensitivity to grid distortions. Second, it provides appropriate approximations in the case of full anisotropic permeability (diffusion) tensor. Third, being combined with the cell-centered FV method, it preserves solution non-negativity and thus provides a monotone discretization.

The two-point flux discretization methods are technologically appealing due to the compact stencil even on polygonal or polyhedral meshes. For cubic meshes and a diagonal diffusion tensor this stencil reduces to the conventional 7-point stencil. We note that for non-orthogonal grids the minimal compact stencil can be guaranteed only for model diffusion or convection-diffusion grid operators but not for discrete Jacobians in multiphase black-oil model.

Since the method is applicable to arbitrary polyhedral grids and multiphase flows with front propagation, the dynamically adapted grids, like octree-based, may be an efficient solution. However, the use of dynamically adapted octree grids rises several issues: time step restrictions, criterion for refinement, data interpolation, grid non-conformity.

The paper outline is as follows. In the second section we recall the black oil model formulation and the

basic ideas of the Newton method and Jacobian matrix assembling. In the third section we remind briefly the nonlinear finite volume scheme and the way of using it for the Jacobian matrix. In the fourth section we summarize the properties of the nonlinear scheme and present a few numerical examples for the two- and three-phase flows. In the fifth section we present the key ideas of implementing octree-based grids for multiphase flows and also present numerical experiments.

Black-oil model

We consider the black oil model in a porous medium Chen et al. (2006). Subscripts denote to the three phases – water, oil (the liquid phase) and gas (the gaseous phase) – and the three components respectively – water, oil and gas.

The basic equations for the black oil model are the following:

1. Mass conservation equations:

$$\frac{\partial}{\partial t}\Big(\phi\rho_w S_w\Big) = -\mathrm{div}\Big(\rho_w \mathbf{u}_w\Big) + \rho_w q_{W_s} \tag{1}$$

for the water component,

$$\frac{\partial}{\partial t}\Big(\phi\rho_{O_o} S_o\Big) = -\mathrm{div}\Big(\rho_{O_o} \mathbf{u}_o\Big) + \rho_{O_o} q_{O_s} \tag{2}$$

for the oil component, and

$$\frac{\partial}{\partial t}\Big[\phi\Big(\rho_g S_g + \rho_{G_o} S_o\Big)\Big] = -\mathrm{div}\Big(\rho_g \mathbf{u}_g + \rho_{G_o}\mathbf{u}_o\Big) + \rho_g q_{G_s} + \rho_{G_o} q_{O_s} \tag{3}$$

for the gas component.

2. Darcy's law for each phase:

$$\mathbf{u}_\alpha = -\frac{k_{r\alpha}}{\mu_\alpha}\mathbf{K}\Big(\nabla p_\alpha - \rho_\alpha \mathbf{g}\nabla z\Big), \quad \alpha = w,o,g. \tag{4}$$

3. The saturation constraint:

$$S_w + S_o + S_g = 1. \tag{5}$$

4. Pressure difference between phases is given by capillary pressure:

$$p_o - p_w = p_{cow}, \qquad p_g - p_o = p_{cgo}, \tag{6}$$

where $\mathbf{K}$ is an absolute permeability tensor, ϕ is a porosity, p_α, S_α, $\mathbf{u}_\alpha$ are *unknown* pressure, saturation and volumetric velocity, μ_α and $k_{r\alpha}$ are the viscosity and relative phase permeability for the phase $\alpha = w,o,g$. Also ρ_w, ρ_{O_o}, ρ_{G_o} and ρ_g are the densities at current conditions, z is the depth, $\mathbf{g}$ is a gravity term, q_{β_s} is a source/sink well term of the component $\beta = W,O,G$ at standard conditions.

We choose oil pressure p_o, water saturation S_w and gas saturation S_g as primary unknowns and take into account the following dependencies. Capillary pressures and relative permeabilities depend on the saturations, $p_{cow} = p_{cow}(S_w)$, $p_{cgo} = p_{cgo}(S_g)$, $k_{r\alpha} = k_{r\alpha}(S_\alpha)$, while porosity, viscosities and densities depend on the pressure, $\phi = \phi^0(1 + c_R(p_o - p_o^0))$, $\mu_\alpha = \mu_\alpha(p_o)$, $\rho_w(p) = \rho_{W_s}/B_w(p_o)$, $\rho_g(p) = \rho_{G_s}/B_g(p_o)$ and $\rho_o = \rho_{O_o}(p_o) + \rho_{G_o}(p_o)$, where $\rho_{O_o}(p) = \rho_{O_s}/B_o(p_o)$, $\rho_{G_o}(p) = R_{so}(p)\rho_{G_s}/B_o(p_o)$, ρ_{β_s} is the component β density at standard conditions and c_R is the rock matrix compressibility constant.

We consider no-flow (homogeneous Neumann) condition on the reservoir boundary. The Peaceman formula suggested in Peaceman (1978) is used for wells with a given bottom hole pressure or flux. For a cell T with center $\mathbf{x}_T$ connected to the well we have:

$$q_{\beta_s} = \frac{k_{r\alpha}}{\mu_\alpha} WI \Big(p_{bh} - p_\alpha - \rho_\alpha \mathbf{g}(z_{bh} - z) \Big) \delta(\mathbf{x} - \mathbf{x}_T), \tag{7}$$

WI is the *well index* which does not depend on the properties of fluids, but depends on properties of the media, $\delta(\mathbf{x} - \mathbf{x}_T)$ is the Dirac function.

The mass conservation equations (1)–(3) are discretized fully implicitly in time:

$$\frac{(\phi \rho_w S_w)^{n+1} - (\phi \rho_w S_w)^n}{\Delta t^{n+1}} = -\mathrm{div}(\rho_w \mathbf{u}_w)^{n+1} + (\rho_w q_{W_s})^{n+1}, \tag{8}$$

$$\frac{(\phi \rho_o S_o)^{n+1} - (\phi \rho_o S_o)^n}{\Delta t^{n+1}} = -\mathrm{div}(\rho_o \mathbf{u}_o)^{n+1} + (\rho_{O_o} q_{O_s})^{n+1}, \tag{9}$$

$$\frac{(\phi \rho_g S_g + \phi \rho_{G_o} S_o)^{n+1} - (\phi \rho_g S_g + \phi \rho_{G_o} S_o)^n}{\Delta t^{n+1}} = -\mathrm{div}(\rho_g \mathbf{u}_g + \rho_{G_o} \mathbf{u}_o)^{n+1} + (\rho_g q_{G_s} + \rho_{G_o} q_{O_s})^{n+1}. \tag{10}$$

Now we can define the nonlinear residual for the l^{th} approximation to a quantity evaluated at time step $n+1$ inside grid cell T_i:

$$R^l_{w,i} = \int_{T_i} \left[\frac{1}{\Delta t^{n+1}} \Big((\phi \rho_w S_w)^l - (\phi \rho_w S_w)^n \Big) + \mathrm{div}\,(\rho_w \mathbf{u}_w)^l - (\rho_w q_{W_s})^l \right] \mathrm{d}x, \tag{11}$$

$$R^l_{o,i} = \int_{T_i} \left[\frac{1}{\Delta t^{n+1}} \Big((\phi \rho_{O_o} S_o)^l - (\phi \rho_{O_o} S_o)^n \Big) + \mathrm{div}\,(\rho_{O_o} \mathbf{u}_o)^l - (\rho_{O_o} q_{O_s})^l \right] \mathrm{d}x, \tag{12}$$

$$R^l_{g,i} = \int_{T_i} \left[\frac{1}{\Delta t^{n+1}} \Big((\phi \rho_g S_g + \phi \rho_{G_o} S_o)^l - (\phi \rho_g S_g + \phi \rho_{G_o} S_o)^n \Big) + \right.$$
$$\left. + \mathrm{div}(\rho_g \mathbf{u}_g + \rho_{G_o} \mathbf{u}_o)^l - (\rho_g q_{G_s} + \rho_{G_o} q_{O_s})^l \right] \mathrm{d}x. \tag{13}$$

The discrete counterpart of (8)-(10) for all grid cells can be written as:

$$R_{\alpha,i} = 0, \quad \alpha = w, o, g. \tag{14}$$

The combination of (4), (14) and (11)-(13) generates a nonlinear system which is usually solved by Newton method:

$$J(x^l)\delta x^l = -R(x^l), \qquad x^{l+1} = x^l + \delta x^l,$$

where l is the l^{th} Newton step, $x = (p_o \;\; S_w \;\; S_g)^T$ is a vector of primary unknowns in all grid cells, $R(x) = \big(R_w(x) \;\; R_o(x) \;\; R_g(x)\big)^T$ is a vector of nonlinear residuals in all grid cells, and J is the Jacobian matrix:

$$J(x) = \begin{pmatrix} \frac{\partial R_w}{\partial p_o}(x) & \frac{\partial R_w}{\partial S_w}(x) & \frac{\partial R_w}{\partial S_g}(x) \\ \frac{\partial R_o}{\partial p_o}(x) & \frac{\partial R_o}{\partial S_w}(x) & \frac{\partial R_o}{\partial S_g}(x) \\ \frac{\partial R_g}{\partial p_o}(x) & \frac{\partial R_g}{\partial S_w}(x) & \frac{\partial R_g}{\partial S_g}(x) \end{pmatrix}.$$

We terminate Newton method when the norm of the residual vector drops below ε_{nwt}.

For the sake of simplicity we only consider water phase terms of the Jacobian since the other are derived similarly. We divide the residual into three parts: accumulation, well and transport terms, $R_{w,i} = R^{acc}_{w,i} + R^{well}_{w,i} + R^{trans}_{w,i}$, where:

$$R^{acc}_{w,i} = V_i \Big((\phi \rho_w S_w)^{l,i} - (\phi \rho_w S_w)^{n,i} \Big), \qquad R^{well}_{w,i} = -\int_{T_i} q^{l,i}_w dx, \qquad R^{trans}_{w,i} = \Delta t^{n+1} \int_{T_i} \mathrm{div}\,\mathbf{u}^l_w \,\mathrm{d}x.$$

While the variation of the accumulation and well terms is straightforward and is defined by (7) and the dependencies given above, the transport term variation highly depends on the the Darcy's fluxes spatial discretization.

Nonlinear FV scheme for Jacobian matrix

We use the finite volume method for spatial discretization. First we remind the nonlinear monotone two-point flux discretization scheme. Let us consider only one conservative unknown c and its flux $\mathbf{q} = -\mathbf{K}\nabla c$.

The FV scheme requires to define the normal component $\mathbf{q}_f^h \cdot \mathbf{n}_f$ of the average flux density $\mathbf{q}_f$ for faces f of the polyhedral grid $\mathscr{T}$. For each cell $T \in \mathscr{T}$, we assign one degree of freedom, C_T, for unknown c. Let C be the vector of all discrete unknowns. If two cells T_+ and T_- have a common face f, our two-point flux approximation, is as follows:

$$\mathbf{q}_f^h \cdot \mathbf{n}_f = D_f^+ C_{T_+} - D_f^- C_{T_-}, \tag{15}$$

where D_f^+ and D_f^- are some coefficients and $C_\pm$ (or $C_{T_\pm}$) be the values of the discrete unknown c in $T_\pm$. We also assume that $\mathbf{n}_f$ is outward for T_+. In a linear FV method, these coefficients are equal and fixed. In the nonlinear FV method, they may be different and depend on unknowns in surrounding cells.

Let $\mathscr{F}_T$ denote the set of faces f of polyhedron T, $\mathbf{x}_T$ denote the collocation point at the barycenter of T, and $\mathbf{x}_f$ denote the barycenter of face f.

For every cell T we define a set Σ_T of nearby collocation points as follows. First, we add to Σ_T the collocation point $\mathbf{x}_T$. Then, for every interior face $f \in \mathscr{F}_T$, we add the collocation point $\mathbf{x}_{T'_f}$, where T'_f is the cell, other than T, that has face f. Finally, for any boundary face $f \in \mathscr{F}_T$, we add the point $\mathbf{x}_f$. Let $N(\Sigma_T)$ denote the cardinality of Σ_T.

We assume that for every cell-face pair $T \to f$, $T \in \mathscr{T}$, $f \in \mathscr{F}_T$, there exist three points $\mathbf{x}_{f,1}$, $\mathbf{x}_{f,2}$, and $\mathbf{x}_{f,3}$ in set Σ_T such that the following condition is held (see Fig. 1): The co-normal vector $\ell_f = \mathbf{K}(\mathbf{x}_f)\mathbf{n}_f$ started from $\mathbf{x}_T$ belongs to the trihedral corner formed by vectors

$$\mathbf{t}_{f,1} = \mathbf{x}_{f,1} - \mathbf{x}_T, \quad \mathbf{t}_{f,2} = \mathbf{x}_{f,2} - \mathbf{x}_T, \quad \mathbf{t}_{f,3} = \mathbf{x}_{f,3} - \mathbf{x}_T, \tag{16}$$

and

$$\frac{1}{|\ell_f|}\ell_f = \frac{\alpha_f}{|\mathbf{t}_{f,1}|}\mathbf{t}_{f,1} + \frac{\beta_f}{|\mathbf{t}_{f,2}|}\mathbf{t}_{f,2} + \frac{\gamma_f}{|\mathbf{t}_{f,3}|}\mathbf{t}_{f,3}, \tag{17}$$

where $\alpha_f \geq 0$, $\beta_f \geq 0$, $\gamma_f \geq 0$. A simple and efficient algorithm for searching a triplet satisfying (17) with non-negative coefficients was presented in Danilov and Vassilevski (2009).

The coefficients α_f, β_f, γ_f are computed as follows:

$$\alpha_f = \frac{D_{f,1}}{D_f}, \qquad \beta_f = \frac{D_{f,2}}{D_f}, \qquad \gamma_f = \frac{D_{f,3}}{D_f}, \tag{18}$$

where

$$D_f = \frac{|\mathbf{t}_{f,1}\ \mathbf{t}_{f,2}\ \mathbf{t}_{f,3}|}{|\mathbf{t}_{f,1}||\mathbf{t}_{f,2}||\mathbf{t}_{f,3}|},\ D_{f,1} = \frac{|\ell_f\ \mathbf{t}_{f,2}\ \mathbf{t}_{f,3}|}{|\ell_f||\mathbf{t}_{f,2}||\mathbf{t}_{f,3}|},$$
$$D_{f,2} = \frac{|\mathbf{t}_{f,1}\ \ell_f\ \mathbf{t}_{f,3}|}{|\mathbf{t}_{f,1}||\ell_f||\mathbf{t}_{f,3}|},\ D_{f,3} = \frac{|\mathbf{t}_{f,1}\ \mathbf{t}_{f,2}\ \ell_f|}{|\mathbf{t}_{f,1}||\mathbf{t}_{f,2}||\ell_f|},$$

and $|\mathbf{a}\ \mathbf{b}\ \mathbf{c}| = |(\mathbf{a}\times\mathbf{b})\cdot\mathbf{c}|$.

For the sake of brevity, we recall formulas for TPFA at interior face f only and isotropic tensor $\mathbf{K}$ only. For more details see Danilov and Vassilevski (2009).

After a few calculations we get the (15) representation of the flux with the non-negative coefficients:

$$D_f^\pm = \mu_\pm |\ell_f| (\alpha_\pm/|\mathbf{t}_{\pm,1}| + \beta_\pm/|\mathbf{t}_{\pm,2}| + \gamma_\pm/|\mathbf{t}_{\pm,3}|). \tag{19}$$

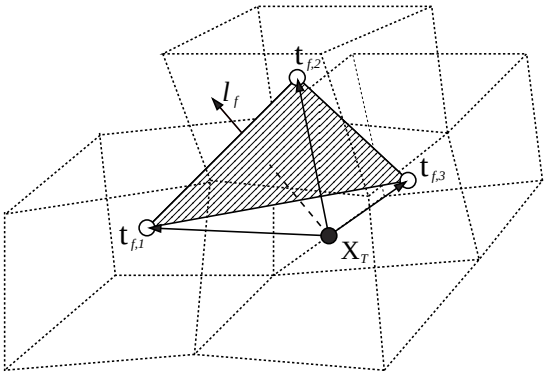

Figure 1 *Co-normal vector and vector triplet.*

The scheme is called nonlinear since the coefficients $\mu_\pm$ and thus $D_f^\pm$ depend on the unknown c:

$$\mu_+ = \frac{d_-}{d_- + d_+} \qquad \text{and} \qquad \mu_- = \frac{d_+}{d_- + d_+}$$

where

$$d_\pm = |\ell_f| \left(\frac{\alpha_\pm}{|\mathbf{t}_{\pm,1}|} C_{\pm,1} + \frac{\beta_\pm}{|\mathbf{t}_{\pm,2}|} C_{\pm,2} + \frac{\gamma_\pm}{|\mathbf{t}_{\pm,3}|} C_{\pm,3} \right). \tag{20}$$

If $d_\pm = 0$, we set $\mu_+ = \mu_- = 1/2$.

Further we need a variation of $D_f^\pm$ to calculate Jacobian matrix. First we write variations for $d_\pm$ and $\mu_\pm$:

$$\Delta d_\pm = |\ell_f| \left(\frac{\alpha_\pm}{|\mathbf{t}_{\pm,1}|} \Delta C_{\pm,1} + \frac{\beta_\pm}{|\mathbf{t}_{\pm,2}|} \Delta C_{\pm,2} + \frac{\gamma_\pm}{|\mathbf{t}_{\pm,3}|} \Delta C_{\pm,3} \right), \tag{21}$$

$$\Delta \mu_\pm = \frac{\Delta d_\mp}{d_\mp + d_\pm} - (\Delta d_\mp + \Delta d_\pm) \frac{d_\mp}{(d_\mp + d_\pm)^2}. \tag{22}$$

Then for the variation of $D^\pm$ we have the linear combination:

$$\Delta D^\pm = \Delta \mu_\pm \left(\alpha_\pm / |\mathbf{t}_{\pm,1}| + \beta_\pm / |\mathbf{t}_{\pm,2}| + \gamma_\pm / |\mathbf{t}_{\pm,3}| \right) = \sum_{T_i \in \Sigma_{T_*}} L_i^\pm \Delta C_i, \tag{23}$$

where $\Sigma_{T_*} := \Sigma_{T_+} \cup \Sigma_{T_-}$ and $L_i^\pm = L_i^\pm(C)$ are the coefficients of the linear combination obtained by substituting (21) and (22) into (19).

Now we split Darcy's fluxes (4) into several parts depending on the primary unknowns p_o, S_w, S_g and depth z:

$$\mathbf{u}_w = -\frac{k_{rw}}{\mu_w} \mathbf{K} \nabla p_o + \frac{k_{rw}}{\mu_w} \mathbf{K} \nabla p_{cow}(S_w) - \frac{k_{rw}}{\mu_w} \mathbf{K} \rho_w \mathbf{g} \nabla z. \tag{24}$$

We apply two-point flux approximation for the flux of each field: p_o, $p_{cow}(S_w)$, $p_{cgo}(S_g)$, z and denote the respective flux coefficients by $D_{p_o}^\pm$, $D_{p_{cow}}^\pm$, $D_{p_{cgo}}^\pm$, $D_z^\pm$ and the collocated field values at $\mathbf{x}_{T_\pm}$ by $p_o^\pm$, $p_{cow}^\pm$, $p_{cgo}^\pm$, $z^\pm$.

If we use the two-point discretization of the flux, then

$$\rho_w \mathbf{u}_{w,f}^h \cdot \mathbf{n}_f = -\left(\frac{\rho_w k_{rw}}{\mu_w} \right)_f \left[\left(D_{p_o}^+ p_o^+ - D_{p_o}^- p_o^- \right) - \left(D_{p_{cow}}^+ p_{cow}^+ - D_{p_{cow}}^- p_{cow}^- \right) - \left(D_z^+ \rho_w \mathbf{g}\, z^+ - D_z^- \rho_w \mathbf{g}\, z^- \right) \right],$$

where term $\frac{\rho_w k_{rw}}{\mu_w}$ for face f is taken upwinded both for pressure and saturation which are denoted by $\widetilde{p}_o$ and $\widetilde{S}_w$, respectively.

Variation of the transport terms can be presented as follows:

$$\Delta(\rho_w \mathbf{u}^h_{w,f} \cdot \mathbf{n}_f) = -\left(k_{rw}\frac{d}{dp_o}\left(\frac{\rho_w}{\mu_w}\right)\right)_f \mathscr{D}_{w,f}\,\Delta\widetilde{p}_o - \left(\frac{dk_{rw}}{dS_w}\frac{\rho_w}{\mu_w}\right)_f \mathscr{D}_{w,f}\,\Delta\widetilde{S}_w -$$

$$-\left(\frac{\rho_w k_{rw}}{\mu_w}\right)_f \left[D^+_{p_o}\Delta p^+_o - D^-_{p_o}\Delta p^-_o + \Delta D^+_{p_o} p^+_o - \Delta D^-_{p_o} p^-_o\right] +$$

$$+\left(\frac{\rho_w k_{rw}}{\mu_w}\right)_f \left[D^+_{p_{cow}}\left(\frac{dp_{cow}}{dS_w}\right)_{T_+}\Delta S^+_w - D^-_{p_{cow}}\left(\frac{dp_{cow}}{dS_w}\right)_{T_-}\Delta S^-_w + \Delta D^+_{p_{cow}} p^+_{cow} - \Delta D^-_{p_{cow}} p^-_{cow}\right] +$$

$$+\left(\frac{\rho_w k_{rw}}{\mu_w}\right)_f \left[D^+_z\left(\frac{d\rho_w}{dp_o}\right)_{T_+}\mathbf{g}\,z^+\Delta p^+_o - D^-_z\left(\frac{d\rho_w}{dp_o}\right)_{T_-}\mathbf{g}\,z^-\Delta p^-_o\right],$$

where $\mathscr{D}_{w,f} = \left[\left(D^+_{p_o}p^+_o - D^-_{p_o}p^-_o\right) - \left(D^+_{p_{cow}}p^+_{cow} - D^-_{p_{cow}}p^-_{cow}\right) - \left(D^+_z\rho_w\mathbf{g}\,z^+ - D^-_z\rho_w\mathbf{g}\,z^-\right)\right]$.

The approximation of the Darcy flux in (4) is obtained by the conventional linear two-point flux discretization or by the nonlinear discretization. In the case of **K**-orthogonal mesh the conventional linear scheme takes the form of the central finite difference and approximates the flux with at least first order accuracy. In general case, the linear scheme may not provide approximation at all.

For the case of nonlinear flux discretization coefficients $D^\pm_*$ must be differentiated as dependent on pressure and saturation in a few neighbouring cells as it was shown in Terekhov and Vassilevski (2013). Therefore,

$$\Delta D^\pm_{p_o} = \sum_{T_i\in\Sigma_{T_*}} L^\pm_{p_o,i}\Delta p^i_o,$$

$$\Delta D^\pm_{p_{cow}} = \sum_{T_i\in\Sigma_{T_*}} L^\pm_{p_{cow},i}\left(\frac{dp_{cow}}{dS_w}\right)^i \Delta S^i_w,$$

$$\Delta D^\pm_{p_{cgo}} = \sum_{T_i\in\Sigma_{T_*}} L^\pm_{p_{cgo},i}\left(\frac{dp_{cgo}}{dS_g}\right)^i \Delta S^i_g,$$

where $L^\pm_{p_o,i}$, $L^\pm_{p_{cow},i}$ and $L^\pm_{p_{cgo},i}$ are the coefficients calculated in (23) for fields p_o, $p_{cow}(S_w)$ and $p_{cgo}(S_g)$, respectively. This results in more dense Jacobian matrix and more expensive Jacobian-vector multiplication and preconditioning in the linear solve.

Properties of the nonlinear scheme

The goal of this section is to summarize the main properties of the nonlinear monotone two-point flux approximation.

It was proved in Danilov and Vassilevski (2009) for diffusion problem that the numerical solution is non-negative if the source term and the initial guess are non-negative. The method is applicable to full anisotropic heterogeneous diffusion tensors and the numerical experiments demonstrate the second-order convergence for the scalar unknown and the first order convergence for the flux variable (a) on unstructured polyhedral meshes and meshes with moderate aspect ratios and (b) for problems with highly anisotropic coefficients.

The application of the new scheme to two-phase flows was studied in Nikitin et al. (2013). For **K**-orthogonal grids all discretizations considered there are identical. However, in case of **K**-non-orthogonal grids the nonlinear TPFA provides more accurate and physically relevant front propagation and water breakthrough time than the conventional linear TPFA. The computational complexity of the new method for fully implicit time stepping scheme is greater than that of the linear TPFA and lesser than that of the MPFA (O-scheme): Table 1 presents number of non-zero elements in Jacobian matrix, CPU time, total

Scheme	nz	time		#nit	#lit
lin.TPFA	229 376	205.67s	1.0x	653	15 896
nonl.TPFA	367 868	343.75s	1.67x	664	23 924
MPFA	893 632	833.64s	4.05x	660	26 288

Table 1 *Sample problem: total number of non-zero elements (nz) in Jacobian matrix, CPU time (sec), total number of nonlinear (#nit.) and linear (#lit.) iterations for simulations with linear TPFA, nonlinear TPFA and MPFA schemes.*

number of nonlinear and linear iterations for 200 days simulation of a sample two-phase water flooding problem for **K**-non-orthogonal grid using the conventional linear TPFA, the nonlinear monotone scheme and the O-scheme MPFA.

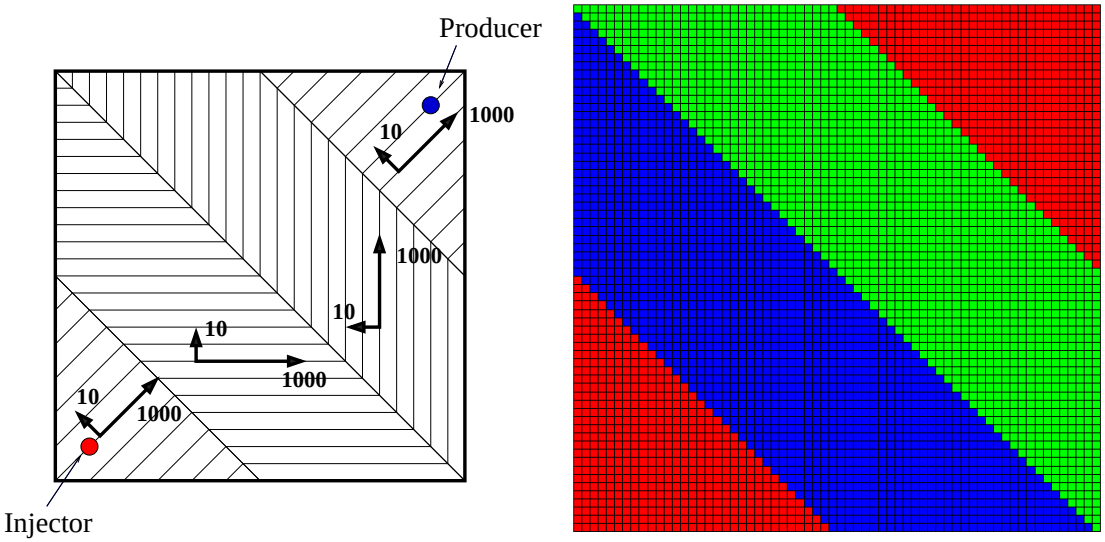

Figure 2 *Left: discontinuous anisotropic tensor. Right: sample mesh.*

The linear TPFA may produce wrong solutions due to the lack of approximation. To compare the linear and nonlinear TPFA schemes we consider the three-phase generalization of the discontinuous anisotropic tensor test case (see Fig. 2) presented in Nikitin et al. (2013). Fig. 3 demonstrates the water and gas saturations at $T = 30$ days for linear and nonlinear TPFA discretizations. One can see that only the nonlinear scheme provides the solution satisfying the media anisotropy directions.

Application on dynamic grids

As the nonlinear scheme provides flux approximation for arbitrary polyhedral meshes, we may use grids based on the octree structure. The key idea here is to treat an octree cell as a polyhedron instead of a cube. This results in a larger stencil for Jacobian matrix since some cells have more than 6 neighbours. On the other hand the octree structure allows us to dynamically refine and coarsen the mesh. To support the process of local refinement and coarsening of the mesh, we use additional structure that represents an octree and stores connections between parents, children and vertices in an octree. Each cubic leaf of an octree can be further split into cut-cells for better approximation of the material layers (see Chernyshenko (2013b)). An example for octree-refined grid with cut-cells is presented on Fig. 4.

The algorithm of dynamic reconstruction consists of a few steps. At first we unite all the cell data from children to parents. Next we unite cells which should be united. Then we find cells which should be refined and refine them. If we need to reconstruct a cell we erase its sub-cells. After an octree structure reconstruction we can cut the updated cells and define data on them.

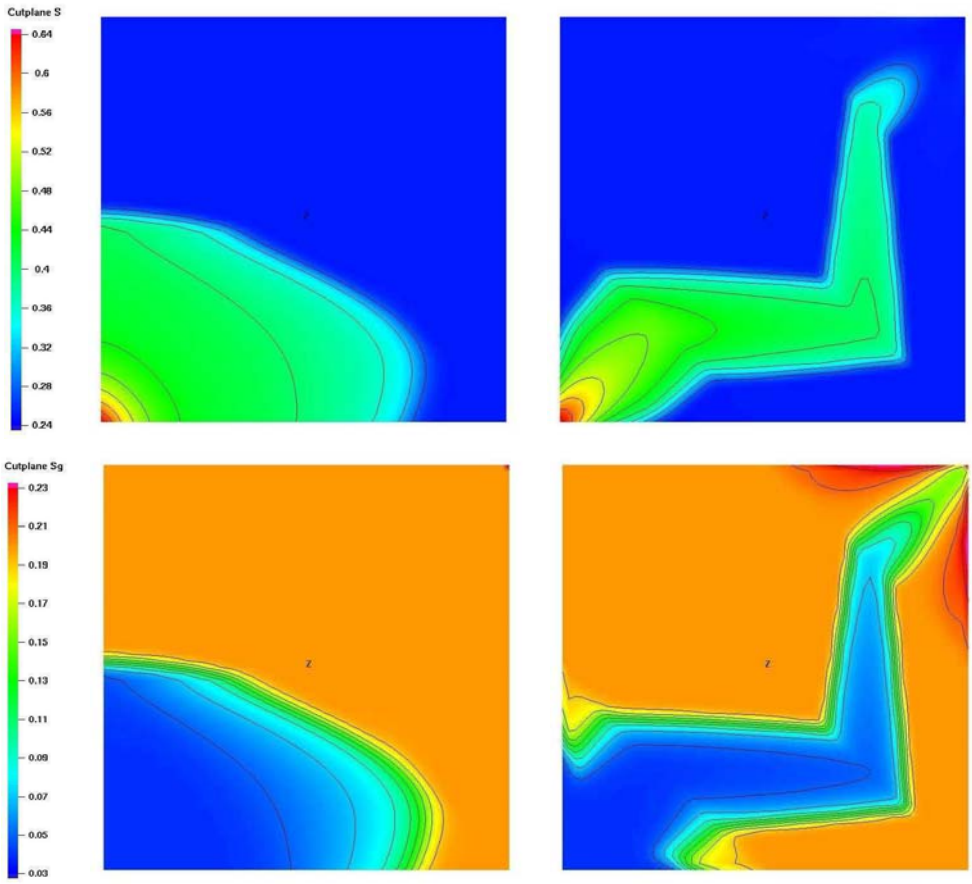

Figure 3 *Isolines for water (top) and gas (bottom) saturations at $T = 30$ days. Discontinuous anisotropic tensor.*

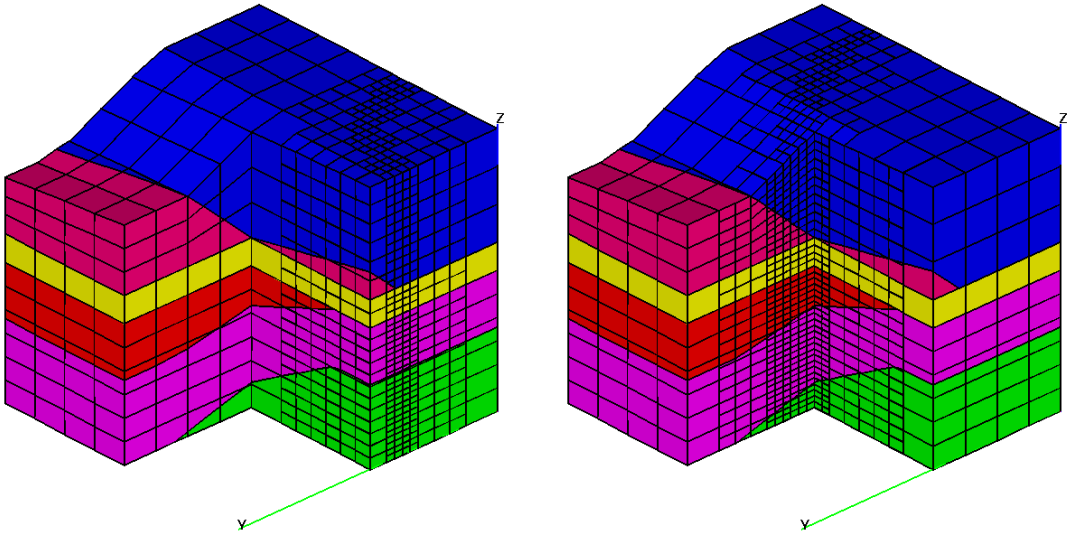

Figure 4 *Sample sequence of dynamically reconstructed meshes with cut-cells.*

Now we demonstrate the performance of the simulation on static and dynamic meshes. We consider two-phase flow for quarter of the five-spot problem with 2 wells and full anisotropic permeability tensor:

$$\mathbf{K}(x,y,z) = R_{xy}(45^o) \cdot \mathrm{diag}(1000, 100, 50) \cdot R_{xy}(-45^o).$$

We choose an *a priori* refinement criteria based on physical properties of field variables. For every material we first calculate the mean $\left(\int_{\Omega_M}|\nabla u|dV\right)/V_{\Omega_M}$ and the maximum $\max_{\Omega_M}(|\nabla u|)$ of the absolute value of the gradient of field variable u, as Ω_M is the part of domain filled with material M. Given a face with two neighbouring cells T_1, T_2 within the same material M, we calculate gradient of field variable u by $|u_1-u_2|/|\mathbf{x}_1-\mathbf{x}_2|$.

Then for an octree leaf cell with a calculated mean absolute value of the gradient $|\widetilde{\nabla u^{n+1}}|_M$, we check it against

$$|\widetilde{\nabla u^{n+1}}|_M \geq \left(\frac{\int_{\Omega_M}|\nabla u^{n+1}|dV}{V_{\Omega_M}}\right)\times(1-tol)+\max_{\Omega_M}|\nabla u^{n+1}|\times tol, \tag{25}$$

where $v^{n+1}=v^n\times(1+\tau)-v^{n-1}\tau$, $\tau=\dfrac{\Delta t^n}{\Delta t^{n-1}}$, tol is a selected parameter. If inequality holds true, then we refine the grid, otherwise we coarsen it. The physical meaning behind the criterion is the following. Setting tol to 1 means that we are interested in the sharpest gradient of u only. This will refine the grid in small area with the largest gradient and leave it coarse everywhere else. This strategy is best suited for pressure which possesses well singularities. Setting tol to 0 means that we are interested in regions where u forms smeared fronts. This strategy is best suited for saturation.

set	tol_P	tol_S
I	0.015	0.035
II	0.025	0.015
III	0.02	0.01

Table 2 *Dynamic grids refinement criteria.*

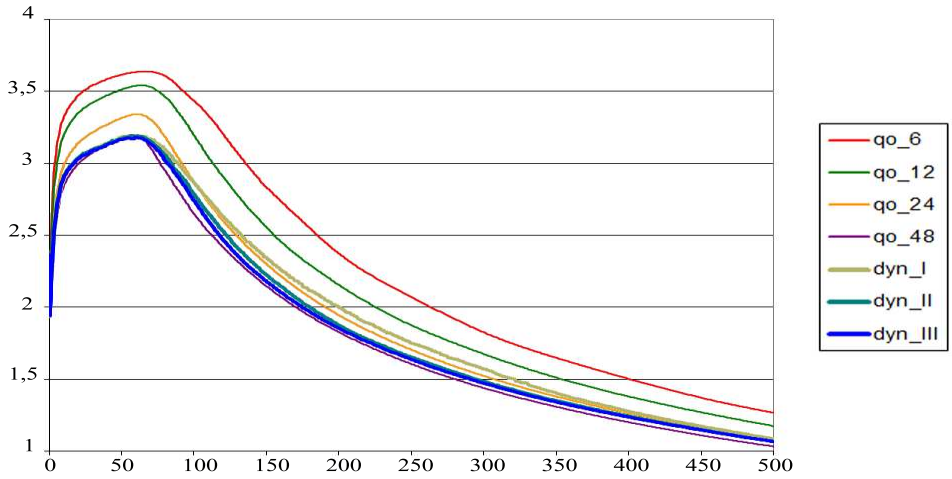

Figure 5 *Oil production rates for static and dynamic grids.*

We compare the solution for three dynamic grids defined by criteria in Table 2 with the one for the uniform $48\times48\times48$ mesh and four static octree meshes with coarsest grid of $6\times6\times6$, $12\times12\times12$, and $24\times24\times24$ and three, two, and one level of refinement to wells, respectively (the mesh step around the wells is the same).

The amount of oil produced is demonstrated in Figure 5. We can see very close results of the simulations on static $48\times48\times48$ mesh and dynamic octree meshes before the water breakthrough. After the water breakthrough we have rather close results as well. From Table 3 we can see the total time of the simulations and the acceleration achieved on the dynamic meshes. The table demonstrates the acceleration up to $4-5$ times on dynamic octree meshes.

mesh	computation,sec	acceleration
$6 \times 6 \times 6$	146	
$12 \times 12 \times 12$	719	
$24 \times 24 \times 24$	4950	
$48 \times 48 \times 48$	45120	1x
dynamic I	9223	4.9x
dynamic II	11815	3.8x
dynamic III	14098	3.2x

Table 3 *Runtime and acceleration for static and dynamic grids.*

Time dependence of the number of mesh elements is shown in Figure 6: octree meshes have the total number of degrees of freedom at most one half of that in the fine uniform mesh.

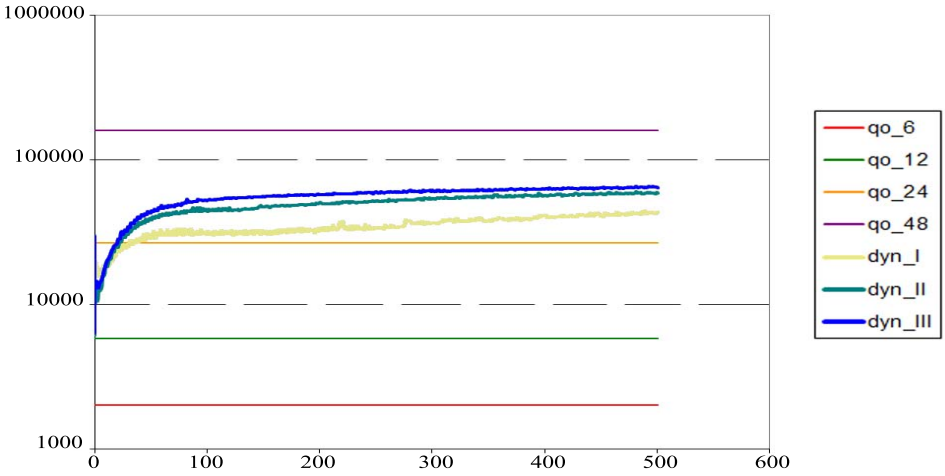

Figure 6 *Number of mesh elements for static and dynamic grids.*

The adapted octree meshes and the water saturations are demonstrated in Figure 7.

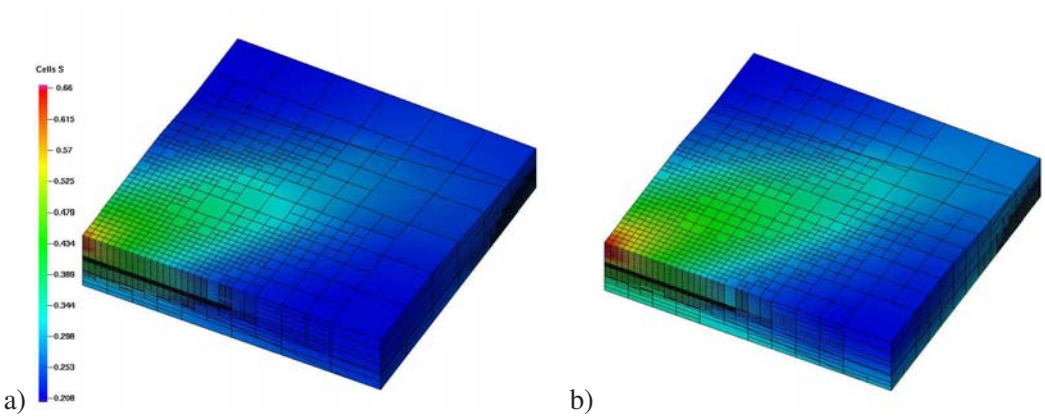

Figure 7 *Water saturation for adapted mesh: a) day 30 b) day 70.*

Conclusions

We considered the application of the nonlinear monotone finite volume scheme to the solution of the two- and three-phase black-oil model problems and dynamically refined polyhedral grids.

The nonlinear scheme has a number of important advantages as well as some disadvantages compared to conventional linear schemes:

- For the linear diffusion problem the scheme is monotone and provides the second order convergence for moderately distorted grids and anisotropic tensors. The stencil is compact, but the nonlinearity of the algebraic system adds complexity to the problem solution.
- For the multiphase flows the scheme provides better accuracy compared to linear TPFA scheme for anisotropic media and non-orthogonal grids. The scheme can no longer be treated as two-point, yet it still has much sparser stencil compared to the linear O-scheme MPFA and thus better computation time.
- The use of dynamically refined grids results in considerable speed-up of simulation with the minimal loss in accuracy at least for two-phase flows simulation.

Acknowledgements

This work has been supported in part by RFBR grants 12-01-33084, 14-01-00830, Russian Presidential grant MK-7159.2013.1, and ExxonMobil Upstream Research Company.

References

Chen, Z., Huan, G. and Ma, Y. [2006] *Computational Methods for Multiphase Flows in Porous Media*. SIAM.

Chernyshenko, A. [2013a] *Generation of adaptive polyhedral meshes and numerical solution of 2nd order elliptic equations in 3D domains and on surfaces*. Ph.D. thesis, INM RAS, Moscow.

Chernyshenko, A. [2013b] Generation of octree meshes with cut cells in multiple material domains. (in russian). *J. Numer. Methods and Programming*, **14**, 229–245.

Danilov, A. and Vassilevski, Y. [2009] A monotone nonlinear finite volume method for diffusion equations on conformal polyhedral meshes. *Russ. J. Numer. Anal. Math. Modelling*, **24**(3), 207–227.

Gao, Z.M. and Wu, J.M. [2013] A small stencil and extremum-preserving scheme for anisotropic diffusion problems on arbitrary 2D and 3D meshes. *J. Comp. Phys.*, **250**, 308–331.

Kapyrin, I.V. [2007] A family of monotone methods for the numerical solution of three-dimensional diffusion problems on unstructured tetrahedral meshes. *Doklady Mathematics*, **76**(2), 734–738.

LePotier, C. [2005] Schema volumes finis monotone pour des operateurs de diffusion fortement anisotropes sur des maillages de triangle non structures. *C. R. Acad. Sci. Paris, Ser. I*, **341**, 787–792.

LePotier, C. [2008] Finite volume scheme satisfying maximum and minimum principles for anisotropic diffusion operators. In: Eymard, R. and Hérard, J.M. (Eds.) *Finite Volumes for Complex Applications*. 103–118.

Lipnikov, K., Svyatskiy, D. and Vassilevski, Y. [2009] Interpolation-free monotone finite volume method for diffusion equations on polygonal meshes. *J. Comp. Phys.*, **228**(3), 703–716.

Lipnikov, K., Svyatskiy, D. and Vassilevski, Y. [2010] A monotone finite volume method for advection-diffusion equations on unstructured polygonal meshes. *J. Comp. Phys.*, **229**, 4017–4032.

Lipnikov, K., Svyatskiy, D. and Vassilevski, Y. [2012] Minimal stencil finite volume scheme with the discrete maximum principle. *Russ. J. Numer. Anal. Math. Modelling*, **27**(4), 369–385.

Nikitin, K., Terekhov, K. and Vassilevski, Y. [2013] A monotone nonlinear finite volume method for diffusion equations and multiphase flows. *Comp. Geosci.*, doi:10.1007/s10596-013-9387-6.

Nikitin, K. and Vassilevski, Y. [2010] A monotone nonlinear finite volume method for advection-diffusion equations on unstructured polyhedral meshes in 3d. *Russ. J. Numer. Anal. Math. Modelling*, **25**(4), 335–358.

Peaceman, D.W. [1978] Interpretation of well-block pressures in numerical reservoir simulation. *SPEJ*, 183–194.

Terekhov, K. and Vassilevski, Y. [2013] Two-phase water flooding simulations on dynamic adaptive octree grids with two-point nonlinear fluxes. *Russ. J. Numer. Anal. Math. Modelling*, **28**(3), 267–288.

Yuan, A. and Sheng, Z. [2008] Monotone finite volume schemes for diffusion equations on polygonal meshes. *J. Comp. Phys.*, **227**(12), 6288–6312.

Yuan, G. and Sheng, Z. [2011] The finite volume scheme preserving extremum principle for diffusion equations on polygonal meshes. *J. Comp. Phys.*, **230**(7), 2588–2604.